Position Measurement over Wide Range by Simultaneous Use of Low and High Coherence Light Source

Miloš C. Tomić and Zoran V. Đinović

***Abstract*—In this paper we propose and experimentally demonstrate a new technique for position/displacement measurement using fiber optic interferometry. We simultaneously employ a low- and a high- coherence light source in the same opto-mechanical configuration. The low coherence signal was obtained using a Fizeau receiving interferometer, implemented as an optical glass wedge, accompanied by a linear CCD array. Combining low- and high-coherence parts was possible because we showed that the accuracy of low-coherence based position measurement was better than 50 nm, less than the high coherence signal periodicity. We verify the method in the dynamic range of low-coherence measurement of about 100 μm, while the accuracy of the high-coherence part was about ±1 nm. Thus, the method provides more than 100,000 measuring points. The advantages of this sensing technique include absolute position/displacement measurement in a large dynamic range with nanometer accuracy.**

***Index Terms*—fiber-optics, interferometry, measurement, sensors**

Original Research Paper
DOI: 10.7251/ELS1519074T

I. Introduction

POSITION and/or displacement measurement is probably the most often measured physical parameter in measurement science and technology. There are many different approaches (e.g. inductive, capacitive, ultrasound, etc.), which have found application in industrial sensors and transducers. However, the use of certain sensor/transducer type is always determined with environmental conditions at the measuring place. A big challenge is the measurement of physical and chemical parameters in harsh environments, or those characterized with specific technical requirements, where sensors must ensure electro-magnetic induction (EMI) immunity, be explosion proof, corrosion resistant, have small size and mass, etc. Of course, it is assumed that such devices have high accuracy, large dynamic range, high measuring rate, high reliability, etc. Beside in common processing industry, such features are very often encountered in aircraft and automotive industry and particularly in medicine.

Optical sensors generally can fulfill most of the aforementioned demands. However, the use of bulk optical components, such as mirrors, lenses, gratings, etc. is unavoidably accompanied by impairment of the initial sensor performance due to contamination build-up and opto-mechanical misalignment caused by thermal and vibrational influences. Fiber-optic sensors, being all-dielectric, very flexible and small in dimensions, offer a number of advantageous solutions capable to overcome these drawbacks [1, 2]. Such an example is the application of fiber-optic sensing technology in optical coherence tomography (OCT), as a novel imaging technology in modern clinical laboratories. OCT provides high-resolution cross-sectional images of the internal microstructure of living tissue. In the skin and other highly scattering tissues, OCT can image small blood vessels and other structures as deep as 1–2 mm beneath the surface with axial resolution of <15μm [3, 4]. Although this resolution is one to two orders of magnitude higher than that of a conventional ultrasound image, there is still room for improvements. At the heart of the system is a fiber-optic position sensor based on low-coherence interferometry with mechanical scanner on the receiving side that limits overall sensitivity of OCT. Our approach, presented in this study, generally aims toward optimization of fiber-optic position/displacement senor, bearing in mind practical applications such as OCT.

Basically, interferometry is one of the most accurate measuring techniques for position/displacement measurement in subnanometer range. A conventional interferometric sensor utilizes a monochromatic, high-coherence light source such a laser or laser diode. However, the output signal of such a sensor is periodic in nature and consequently limits the unambiguous measuring range. This range can be extended by some accompanying techniques such as the two-wavelengths interferometry, tunable light source or quadrature signals [5-7]. Nevertheless, in all these cases, periodicity of the cosine function causes ambiguity in absolute position determination with a period of quarter of wavelength. It can be overcome by the conventional fringe-counting technique, but the initialization problem still remains. Low-coherence interferometry [8, 9], on the other hand, overcomes the problem of absoluteness and initialization since it generates an

Manuscript received 08 November 2015. Received in revised form 15 December 2015.

This work was financially supported by the Austrian Science Fund (FWF) within the framework of the Project L139-N02 "Nanoscale measurement of physical parameters" and ACMIT Gmbh.

M. C. Tomic is with the School of Electrical Engineering, University of Belgrade, Belgrade, Serbia (e-mail: milos.tomic@gmail.com).

Z. V. Đinović is with ACMIT Gmbh, Wiener Neustadt, Austria.(e-mail: zoran.djinovic@acmit.at).

interferometric pattern with Gaussian shape by mechanical scanning of the optical path at the receiving side. The absolute position can be unambiguously determined with an accuracy of several tenths of nanometers by using some of techniques for finding the center of coherence zone, i.e. the maximum of Gaussian function. However, every movable part in the sensing configuration, either for optical path scanning or/and phase-shifting, is a permanent source of instabilities and inaccuracies. Recently, Zhao et al. [10] reported on a novel absolute displacement measurement technology which completely excludes scanning. It is based on the wavenumber spectrum of low coherence interferometry with a resolution of about 6 nm in a measuring range of 50 μm. Wang et al. [11] achieved measurement resolutions below 1 nm in a range of 6 mm by multiplexing low- and high-coherence fiber-optic interferometric system, also without mechanical scanning.

In this paper we employ both techniques at the same time using a single measuring interferometer and avoiding a mechanical scanner. On the receiving side, we separate the signals belonging to the high- and the low-coherence light sources. It is achieved using different wavelengths for low- and high-coherence sources. The main advantages of this novel technique are relatively low resolution demands in every single evaluation step, either low- or high-coherence. A long-term stable and accurate sensing system is realized by the electronic interrogation of the low-coherence signal by 1D CCD. The high-coherence signal is captured by a photo diode.

II. Principle of Operation

The proposed method is based on the simultaneous use of two in principle different interferometric measurement techniques, low- and high-coherence interferometry. The common part in both techniques is the arrangement at the measurement point, where the measured distance acts as a path imbalance (difference) of the two-beam interferometer. The difference between these two methods is on the receiving side.

The intensity of the combined signal of a two-beam interferometer I_P is equal:

$$I = I_1 + I_2 + 2\sqrt{I_1}\sqrt{I_2}\,|\gamma_{11}(\Delta L_{12})|\cos(2\,\mathrm{k}\,\Delta L_{12}) \qquad (1)$$

where I_1 and I_2 are the intensities of two beams, k is the wavenumber, ΔL_{12} is the path difference and γ_{11} is the light source coherence degree. The product $2k\Delta L_{12}$ is the optical path difference of the interferometer.

When the measuring interferometer is illuminated by a high coherence source, i.e. if $|\gamma_{11}(\Delta L_{12})| \approx 1$, the detection is made by a simple intensity detector. The path difference (i.e. the position) can be measured with a very high precision, especially in the vicinity of the midway between the top and the bottom of the cosine waveform. In order to cover the whole range of one cosine period, more complicated schemes can be used [5-7]. These are mainly based on generation of so called quadrature signals. For instance, one of these methods employs a 3x3 fiber-optic directional coupler [7]. However, in all these cases, the periodicity of the cosine function causes ambiguity in the absolute position determination within the quarter-wavelength period. It can be overcome by the ordinary fringe counting technique, but the initialization problem still remains.

On the other hand, when the measuring interferometer is illuminated by a low coherence source, i.e. when ΔL_{12} is large enough that $\gamma_{11}(\Delta L_{12}) \approx 0$, finding the path difference is more complicated. A second interferometer on the receiving side, the so-called receiving interferometer, should be used. In this way the absolute position can be determined using some of the techniques for finding the center of the coherence zone [12].

In this paper we employ both techniques at the same time, using the same measuring interferometer. On the receiving side, we should be able to separate the signals belonging to the high- and the low-coherence light source. It can be achieved using different wavelengths for two sources, or by fast light switching so that the only one is emitting at one moment. To avoid transient and temperature effects, it is the best practice to utilize fiber optic switches.

We can determine the phase angle of the measuring interferometer φ_{HC} at some instant, starting from the high-coherence signal value and knowing the signal history. The knowledge on the history of the signal changes is necessary because we should always know the interferometric maximum and minimum, in order to determine the inverse function of (1). The measured distance D_{HC} is directly proportional to the phase angle φ_{HC} by

$$D_{HC} = \varphi_{HC} \cdot \frac{\lambda_{HC}}{4\pi} \qquad (2)$$

where λ_{HC} is the wavelength of the high-coherence light source. An additional complication arises from the fact that the cosine function has an additional ambiguity inside the full angle of 2π radians: an angle α and an angle $(2\pi\text{-}\alpha)$ produce the same photodetector signal. Thus, the periodicity of the distance measured by a high-coherence signal, using a single photodetector, equals to a quarter of the employed wavelength.

The position obtained using a low-coherence source is represented by a continuously changing variable, which corresponds to the maximum of the Gaussian envelope of the interferometric signal maxima. This signal is produced by either a spatial pattern, usually a set of parallel fringes, detected by a CCD sensor, or by a photodiode signal in systems employing mechanical scanning. Generally, mechanical scanning techniques have some drawbacks such as low speed and mechanical instabilities which we avoided in this paper. The best choice by far for the receiving interferometer, capable to overcome the aforementioned drawbacks, is a glass wedge, suitable positioned and firmly fixed to the CCD linear array. If the wedge angle is θ, the intensity along the CCD line in the x direction is

$$I = I_1 + I_2 + 2\sqrt{I_1}\sqrt{I_2}\,|\gamma_{11}(\Delta L_{12} + x\sin\theta)|\cos(2\,\mathrm{k}(\Delta L_{12} + x\sin\theta)) \qquad (3)$$

The coherence degree reaches its maximum of unity when its argument is equal to zero; the corresponding position along the CCD array is Xc:

$$\Delta L_{12} + x\, n_W \sin\theta = 0 \rightarrow x = \frac{-\Delta L_{12}}{n_W \sin\theta} \equiv X_C \qquad (4)$$

where θ is the wedge angle and n_W is the index of refraction of the wedge glass.

It is evident from (4) that the optical path difference ΔL_{12} can be determined from the position along CCD where the interferometric fringes have the maximal contrast, X_C. Moreover, the exact position of X_C is the local maximum of intensity, because of the cosine member in (3).

Let us suppose now that we are continuously changing the optical path difference, causing that the center of the low-coherence interferogram is moving along the CCD line, while we are at the same time monitoring the high-coherence phase angle φ_{HC}. In this way, we can establish the list of successive positions $X_C=X_1, X_2,\ldots, X_N$, where the phase angle φ_{HC} abruptly changes its value from π to zero. This procedure is illustrated in Fig.1.

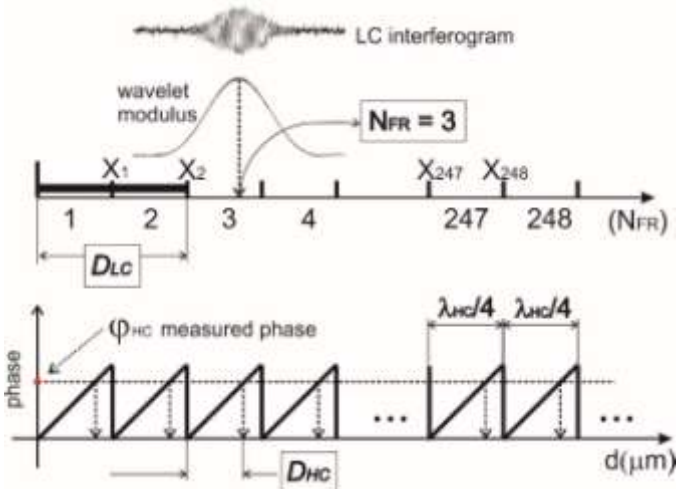

Fig. 1. Principle of interferometric measurement of distance simultaneously using low and high coherence light sources

We now define a set of successive intervals along the CCD array; the intervals are limited by the list members in such a manner that, for instance, the interval N_{FR}=247 is between X_{248} and X_{249}, see Fig. 1 top.

In the measurement method we are proposing here, we firstly find the so-called low-coherence part of the measured distance D_{LC}. Then, employing suitable signal processing, we calculate the position of the interferogram maximum – X_C. Further, the serial number of the CCD interval, corresponding to X_C is determined. This number – N_{FR}, corresponds to the number of the whole high-coherence interferometric fringes from the system zero point. The low-coherence part D_{LC} is equal to

$$D_{LC} = (N_{FR} - 1) \cdot \frac{\lambda_{HC}}{4} \qquad (5)$$

Finally, the measured distance D is equal to the sum of the distances determined from the low- and the high-coherence interferometric signals:

$$D = D_{LC} + D_{HC} = \frac{\lambda_{HC}}{4} \cdot (N_{FR} - 1 + \frac{\varphi_{HC}}{\pi}) \qquad (6)$$

Thus, as seen from (6), we need to determine the two values: one from the low-coherence interferogram – N_{FR}, and another, from the high-coherence interferogram – φ_{HC}.

The first one assures a very large dynamic range of measurement. The range depends primarily on the CCD length and the receiving interferometer wedge angle.

The second value, the high-coherence phase angle, brings high precision to the measurement, limited mostly by the signal-to-noise ratio of the high-coherence interferogram.

The total accuracy depends essentially on our ability to accurately find the true serial number of the interval, i.e. on the signal-to-noise ratio of the low-coherence interferogram and the coherence length of the low-coherence source. It is obviously required that the uncertainty of finding the position of low-coherence interferogram maximum must be far better than a quarter of high-coherence wavelength.

III. Experiment

In Fig. 2 we present a block scheme of the main sensing configuration, based on a Fizeau interferometer illuminated by two light sources of different degrees of coherence. These two sources, one of which emits low-coherence light and the other high-coherence, have also different wavelengths. A pigtailed low-coherence source LCS (superluminescent diode at 850 nm) is connected via two 1x2 fiber-optic couplers (FOC1, FOC3) to one of the input arms of the central 2×2 fiber-optic coupler (FOC4). The silicon photodiode Pd1 is used to monitor the optical power of LCS, using a part of the radiation taken from LCS by FOC1. In the same manner, a high-coherence light source HCS (solid-state laser coupled to the single mode 4/125μm fiber, at 1064 nm) is connected to the same input arm of the FOC4 coupler via a pair of 2x1 couplers. An InGaAs photodiode Pd2 is used to monitor the optical power of HCS, through FOC2. The high- and the low-coherence radiation is combined using the third 2x1 coupler FOC3.

One output arm of FOC4 is directed toward the mirror M which acts as a movable target. The second output arm of FOC4 is immersed in the index-matching gel (MG), in order to suppress back-reflection from the free fiber end. The sensing interferometer of Fizeau type is formed from the fiber end and the mirror M. The gap between these two surfaces - ΔL is the distance we want to measure in this experiment.

The low- and the high-coherence light signal are backreflected at the same time, along the same path, from the fiber end and the mirror. The four reflected waves are combined in the coupler FOC4 and outputted at its second "input" arm. This arm is connected to FOC5, another 1x2 fiber-optic coupler, which splits the four combined beams into two halves.

Since we want to separate the high- and the low-coherence signals, which have different wavelengths, ideally FOC5 should be a wavelength-division-multiplexer (WDM) coupler. However, to be detectable by an ordinary CCD detector, the wavelength of LCS has to be around 850nm. Since the laser is at 1064 nm, and could be at 1310 nm or 1550 nm, this kind of single-mode WDM couplers is not readily available.

In the detection part of the system, another InGaAs photodiode Pd3 is employed for the detection of high-coherence radiation. The low-coherence part of radiation, being at a shorter wavelength, is eliminated by an optical highpass or bandpass filter (LPF) placed in the front of the photodetector. The other arm of FOC5 is directed towards the optical stack intended for low-coherence interferometric demodulation. The stack is composed of a lens, an optical wedge and a linear CCD array. The lens is used to collimate the cone of radiation emerging from the fiber end. The optical wedge is acting as a receiving interferometer of Fizeau type. The CCD array should have as many pixels as possible, those itself should be as small as possible. We used the Panavision CCD linear image sensor ELIS-1024, with 1024 pixels of effective size 7.8 µm x 125 µm. There has been no need for a lowpass optical filter in front of the CCD, because the CCD silicon material is insensitive to wavelengths longer than 1 µm.

We fabricated a series of glass wedges, with different wedge angles, lengths and thicknesses, as custom designed components with Casix [13]. The wedge angles of 0.5°, 1° and 2° were manufactured, with lengths of 10 and 25 mm, and with widths of 3 mm and 0.5 mm. The starting thickness, at the wedge, was generally made as small as possible (about 100 µm). All experiments have been performed by the fiber-optic sensing configuration depicted in Fig. 2, using a wedge with an angle of 0.5º as the receiving interferometer.

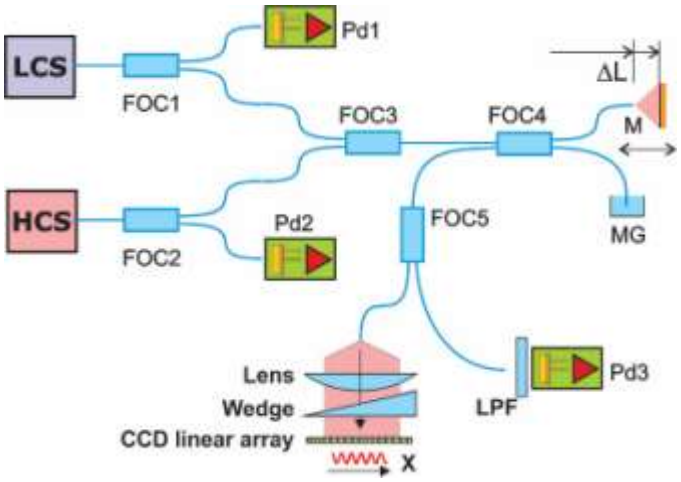

Fig. 2. Experimental configuration for interferometric distance measurement: HCS-high-coherence source, LCS low-coherence source, FOC1-5 – fiber-optic couplers, Pd1-3 photodiodes, LPF-high-pass filter, MG-index matching gel, M-movable mirror acting as target.

We have been using arc splicing to connect all couplers, in order to suppress the phenomenon of back-reflection noise from possible fiber gaps.

An overall view of the sensing part of the measuring set up is presented in Fig. 3. It is composed of a linear DC motorized stage – a Thorlabs production, equipped with an encoder for the position reading with resolution of about 40 nm (not accuracy!). The DC motor is driven by a PI (Physical Instruments) PCI card and software. A PZT transducer with a dynamic range of about 10µm is firmly fixed to the mechanical stage. The PZT transducer is driven by a high voltage amplifier, in order to produce small AC displacements for phase angle reading calibration. An aluminum mirror of 5 mm in diameter was glued to the tip of the PZT transducer. The sensing fiber end was firmly fixed by a standard fiber-optic cannula made of brass in front of the mirror. Measured value was the fiber-optic end vs. mirror distance.

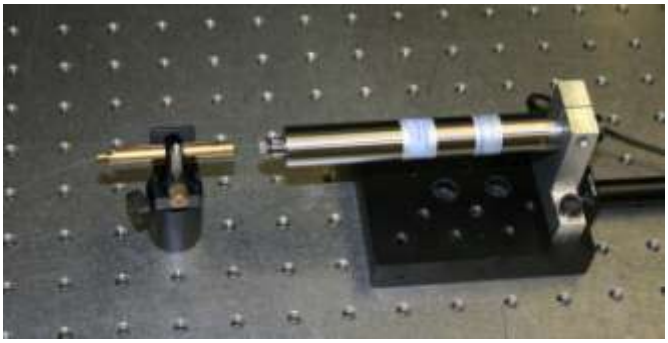

Fig. 3. The sensing Fizeau interferometer: the sensing fiber arm (left) in the brass cannula positioned against Al mirror, mounted on the PZT transducer and DC motorized stage (right)

Large displacements, in the range of 100 µm, were performed by the DC stage. The signal showing the stage position and other signals from photodiodes and CCD array were captured by a National Instruments acquisition card.

The high-coherence signal has continuously been capturing during all measurement time. The low-coherence signal, i.e. particular linear images, has been captured at the discrete moments, after moving the sensing mirror to the new measurement position. The low- and the high-coherence signal acquisition was strictly synchronized in time.

The experiments showed that it was not too difficult to align the parts; the interferometric signals were substantially stable and relatively immune to external vibrations and acoustic disturbances. Temperature effects were also negligible, providing that the joint between the glass wedge and the CCD device was made without any glue (we used the mechanical parts made of MACOR ceramic).

The glass window that covers the CCD surface is factory-assembled and cannot be easily removed. Consequently, it was impossible to bring the glass wedge into a closer contact with the CCD surface, as required for a high visibility of the interferometric fringes. It caused a relatively poor signal-to-noise ratio of the low-coherence signal, increasing the processing time and the measurement uncertainty.

The most important conditions for maintaining a reliable connection between the high- and low-coherence parts of the measurement are simultaneous detection and mechanical stability of all receiving interferometer parts, especially between the glass wedge and the CCD detection array.

IV. Results and Discussion

In Fig. 4 we present a screenshot of a typical raw low-coherence signal, recorded in one particular mirror position. This signal has a characteristic shape of interferometric low-

coherence Gaussian-enveloped pattern, superimposed upon a quasi-DC signal, reflecting the light intensity distribution over the CCD array. In a single experiment, we usually acquired about 20-40 interferometric patterns like this one. Every CCD pattern has been digitized as a set of 1024 12-bit values.

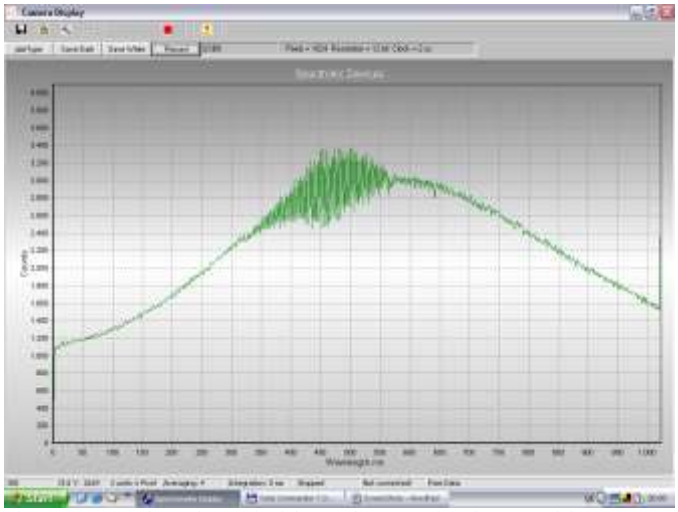

Fig. 4. Screen shot of a typical low-coherence signal captured by 1D CCD EPLIS 1024 sensor array

The raw high-coherence signal, captured by the InGaAs photodiode, is presented in Fig. 5. The shape of the signal clearly reveals a set of discrete positions of the moving mirror during the experiment. These signal portions are bounded by sudden phase changes, caused by the mirror shifts. The mirror has been moved using DC motorized stage, shifting in discrete steps of 4 µm, over the range of about 90 µm.

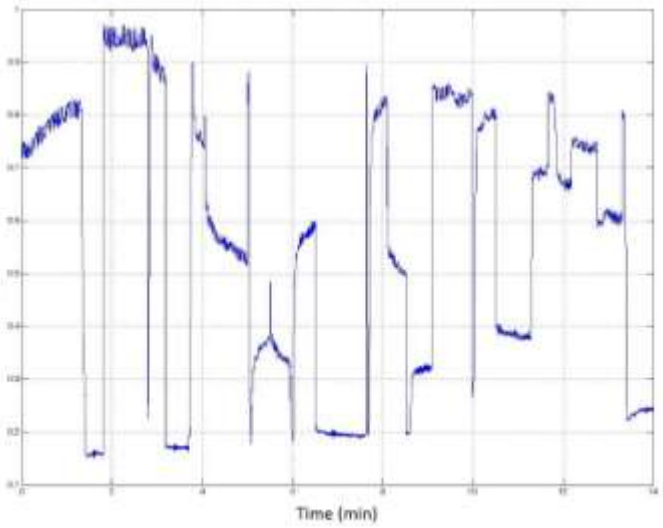

Fig. 5. Raw high-coherence signal during 23 mirror shifts by 4 µm, captured continuously in time of the experiment.

The signal processing of the low coherence signal, performed off-line using Matlab software packet [14], starts with normalization using the CCD signal obtained from the non-interferometric pattern. In this way the influence of non-uniform distribution of optical intensity across the sensing line is eliminated. Then, we applied wavelet transformation, using the complex Morlet 6-10 continuous wavelet [15], which corresponds to the shape of the low-coherence interferogram. The modulus of the appropriate transformation scale was fitted by Gauss function, where the fitting parameter was the position of the center. The half-width and the maximum of Gauss function, being dependent on the low-coherence source coherence length and power, are invariable in the measuring system and known. The best-fit Gauss center is our low coherence position *Xc*, from (4). The values obtained in this way, transformed according to (4), from *Xc* to low-coherence positions, are presented and labeled on the right side of the graph in Fig. 6. These positions show a linear trend over the whole 90 µm range, reflecting the way of the real movement of the mirror in the sensing interferometer.

The high-coherence signal was transformed to a phase angle using the usual interferometry inverse-cosine transformation, based on (1), where the maximum and minimum of the high-coherence signals are unchangeable and known. The calculated phase angle walks in the frame of about 250 nm, corresponding to 1/4 of the laser source wavelength. These values, taken in discrete time moments, are shown and labeled on the left side of the graph in Fig. 6.

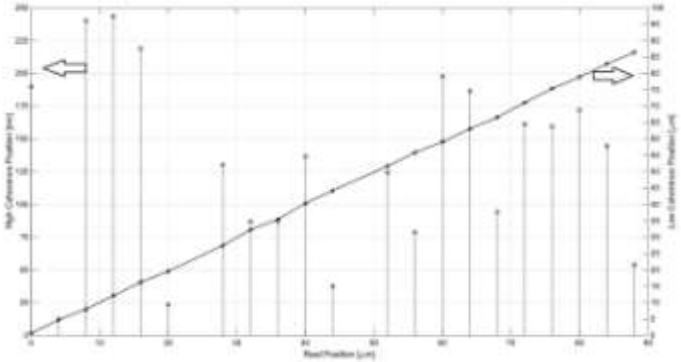

Fig. 6. Combined processed high- and low-coherence signal in the complete measurement range, from zero to 90 µm. The high-coherence signal is calculated from the phase angle taken at moments of capturing the low-coherence signal.

The exact measured position can be calculated by adding the path difference belonging to this phase angle φ_{HC} to the bottom of $\lambda_{LC}/4$ ruler, obtained from the low-coherence position X_C, as explained in Section II. A comparison of calculated and the settled position is not shown here because the accuracy of reading the DC motor position was not good enough for this purpose. This part of method verification is left for the experiments based on a specially prepared step-target, characterized in advance by a profilometer.

The ultimate request for the accuracy of the method is the determination of unambiguity of the absolute target (mirror) position out of the low-coherence signal. For this purpose we recorded the low-coherence signal during about eight minutes, while the mirror was steady in a certain position. The pixel position of center of coherence zone, calculated by fitting using Gauss function, for 41 successive measurements is shown in Fig. 7. The pixel number is not a counting number because the fitting output is a continuous value.

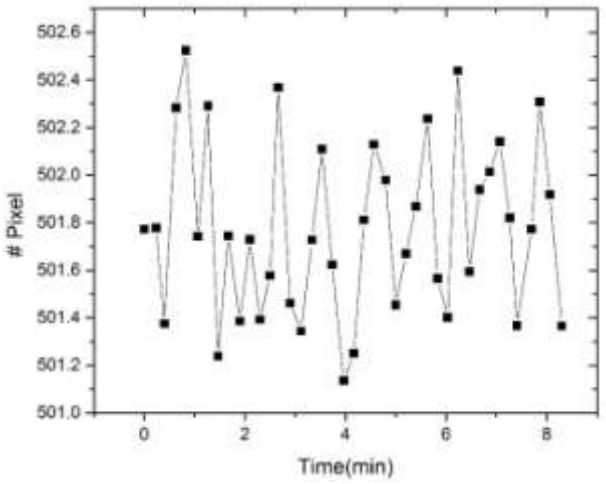

Fig. 7. Change of position of the coherence zone center on CCD, obtained by wavelet signal processing, during about 8 minutes in steady state condition. The position is given in the pixels numbers, used as continuous variable in Gaussian fitting.

The connection between the pixel number value and the real position can be found from the slope of the low-coherence curve in Fig. 6, or from (4). The slope in this experiment was about 100 nm/pixel. The histogram of deviations from the steady position, calculated from 8-minutes data shown in Fig. 7, is presented in Fig. 8.

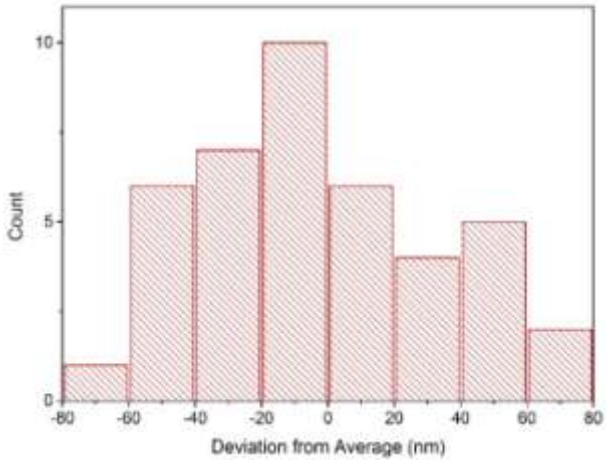

Fig. 8. Histogram of data from Fig.7. transformed into distance units, using the pixel/distance slope found from the low coherence scan presented in Fig.6, Short term repeatability of measurement, indicating the precision of low coherence measurement is about 44 nm (standard deviation).

The standard deviation from the steady – average position is calculated from the data shown in Fig. 8. The deviation is about 44 nm, which means that the probability of misreading the serial number of $\lambda_{HC}/4$ interval is about 0.0065. This result is obtained for a 1064 nm high-coherence wavelength and for a position in the middle of $\lambda_{HC}/4$ interval. The probability of wrong determination of the interval number rises as the calculated low-coherence position approaches the edge of interval, until the unacceptable value of 0.5 is encountered at its very edge. The proximity of the edge can also be recognized if the high- coherence phase angle is close to zero or π. In these cases, additional attention should be paid and the process of determination of the interval serial number should take into account the signal continuity.

V. Conclusion

A new technique for position/displacement measurement has been proposed. The technique simultaneously uses fiber-optic low- and high-coherence interferometry in the same sensing configuration without any scanning mechanism on the receiving side. In this way a nanometer scale accuracy of about ±1 nm and an absolute measurement of target position in a wide dynamic range of about 100 μm is assured and experimentally confirmed. Hence, the technique provides more than 100,000 measuring points in the examined configuration, although much more can be achieved, even more than one million, using a CCD array with a larger number of pixels and a longer glass wedge.

Acknowledgment

This work was financially supported by the Austrian Science Fund (FWF) within the framework of the Project L139-N02 “Nanoscale measurement of physical parameters” and ACMIT Gmbh.

References

[1] K.T.V. Grattan, T. Sun, “Fiber optic sensor technology: an overview”, Sensors and Actuators, vol. 82, pp. 40-61, May 2000
[2] E. Udd, An overview of fiber-optic sensors, Rev. Sci. Instrum, vol. 66, pp. 4415-4030, Aug. 1995
[3] J. G. Fujimoto, J. M. Schmitt, E. A. Swanson, I.-K. Jang, “The development of OCT”, in *Cardiovascular OCT imaging*, I.-K. Jang Ed. New York: Springer 2015, pp. 1-21
[4] J. M. Schmitt, “Optical coherence tomography (OCT): a review, IEEE Journal of Selected Topics in Quantum Electronics, vo.l 5, pp.1205-1215, Jul./Aug.1999 1205
[5] A.D. Kersey, A. Dandrige, W. K. Burns, “Two-wavelength fiber gyroscope with wide dynamic range”, Electron. Lett., vol. 22, pp. 935-937, Aug. 1986
[6] H. Kikuta, K. Iwata, R. Nagata, “Distance measurement by the wavelegth shift of laser diode light”, Appl. Opt., vol. 25, pp. 2976-2980, Sep. 1986
[7] D. A. Brown, C. B. Cameron, R. M. Keolian, D. L. Gardner, S. L. Garrett, “A symmetric 3x3 coupler based demodulator for fiber optic interferometric sensors”, SPIE 1584, Fiber Optic and Laser Sensors IX, 1991, pp. 328-335
[8] Y-J. Rao, D. A. Jackson, “Recent progress in fibre optic low-coherence interferometry”, Measurement Science and Technology, vol. 7, pp. 981-999, Jul. 1996
[9] M. A. Choma, C. Yang, J. A. Izatt, “Instantaneous quadrature low-coherence interferometry with 3 3 3 fiber-optic couplers”, vol. 28, pp. 2162-2164, Nov.2003
[10] K. Zhao, F. Xie, S. Ma,Y. Wang, L. Chen, “A novel absolute displacement measurement technology based on wavenumber resolved low coherence interferometry”, Optics &Laser Technology, vol. 75, pp. 34-39, Dec. 2015
[11] Y. Wang, F. Xie, S. Ma, L. Chen, “Remote and high precision step height measurement with an optical fiber multiplexing interferometric system”, Optics and Lasers in Engineering, vol. 66, pp. 52-57, Mar. 2015
[12] M. C. Tomic, J. M. Elazar, Z. V. Djinovic, “Low-coherence interferometric method for measurement of displacement on a 3x3 fiber-optic directional coupler”, J. Opt. A: Pure Appl. Opt., vol. 4, pp. S381-S386, Nov. 2002
[13] http://www.casix.com/ (assessed 08.11.2015)
[14] MATLAB and Statistics Toolbox Release, The MathWorks, Inc., Natick, Massachusetts, United States, 2012
[15] A. Teolis, “Computational signal processing with wavelets”, Birkhauser, Boston, 1998, pp.65-66